



This item was submitted to Loughborough's Institutional Repository (<https://dspace.lboro.ac.uk/>) by the author and is made available under the following Creative Commons Licence conditions.



CC creative commons
COMMONS DEED

Attribution-NonCommercial-NoDerivs 2.5

You are free:

- to copy, distribute, display, and perform the work

Under the following conditions:

BY: **Attribution.** You must attribute the work in the manner specified by the author or licensor.

Noncommercial. You may not use this work for commercial purposes.

No Derivative Works. You may not alter, transform, or build upon this work.

- For any reuse or distribution, you must make clear to others the license terms of this work.
- Any of these conditions can be waived if you get permission from the copyright holder.

Your fair use and other rights are in no way affected by the above.

This is a human-readable summary of the [Legal Code \(the full license\)](#).

[Disclaimer](#) 

For the full text of this licence, please go to:
<http://creativecommons.org/licenses/by-nc-nd/2.5/>

MAP-MATCHING IN COMPLEX URBAN ROAD NETWORKS

W.Y. Ochieng, M. Quddus
R.B. Noland

Centre for Transport Studies
Department of Civil and Environmental Engineering
Imperial College London, London SW7 2AZ, United Kingdom
w.ochieng@imperial.ac.uk

ABSTRACT

Global Navigation Satellite Systems (GNSS) such as GPS and digital road maps can be used for land vehicle navigation systems. However, GPS requires a level of augmentation with other navigation sensors and systems such as Dead Reckoning (DR) devices, in order to achieve the required navigation performance (RNP) in some areas such as urban canyons, streets with dense tree cover, and tunnels. One of the common solutions is to integrate GPS with DR by employing a Kalman Filter (Zhao et al., 2003). The integrated navigation systems usually rely on various types of sensors. Even with very good sensor calibration and sensor fusion technologies, inaccuracies in the positioning sensors are often inevitable. There are also errors associated with spatial road network data. This paper develops an improved probabilistic Map Matching (MM) algorithm to reconcile inaccurate locational data with inaccurate digital road network data. The basic characteristics of the algorithm take into account the error sources associated with the positioning sensors, the historical trajectory of the vehicle, topological information on the road network (e.g., connectivity and orientation of links), and the heading and speed information of the vehicle. This then enables a precise identification of the correct link on which the vehicle is travelling. An optimal estimation technique to determine the vehicle position on the link has also been developed and is described. Positioning data was obtained from a comprehensive field test carried out in Central London. The algorithm was tested on a complex urban road network with a high resolution digital road map. The performance of the algorithm was found to be very good for different traffic maneuvers and a significant improvement over using just an integrated GPS/DR solution.

Keywords: Global positioning system, Dead-reckoning, Kalman Filter, Map matching, Transport telematics, Intelligent transportation system.

1. INTRODUCTION

A range of transport telematics applications and services such as in-car navigation systems, dynamic route guidance systems, fleet management, collision avoidance systems, advanced traveler information and on-board emission monitoring require continuous accurate positioning information on motor vehicles traveling on the road network. Many services also require real-time display of the vehicle location on a map in an error-free fashion. Two essential components commonly used for such applications and services are, (a) sensors to determine the geometric position of the vehicles, and (b) Geographic Information Systems (GIS) based digital maps for the identification of the physical location of the vehicles. An interesting but challenging problem is to integrate positioning sensor data with digital map data to improve the accuracy with which the vehicle location on a road link is determined.

Common devices used for land vehicle navigation are Dead Reckoning (DR) sensors, ground-based (Terrestrial) radio frequency systems, satellite based radio navigation systems such as GPS, and

integrated navigation systems such as GPS and DR. These state-of-the-art navigation systems usually rely on various types of sensors. Even with very good sensor calibration and sensor fusion technologies, inaccuracies are often inevitable. Moreover, there is also imprecision with GIS-based digital road maps due to plotting errors, map resolution and piece-wise linear links to approximate road curvature. As a result of such inaccuracies in the positioning system and the digital base map, actual geometric vehicle positions do not always map onto the spatial road map, when the vehicle is known to be on the road network. This phenomenon is known as *spatial mismatch*. The spatial mismatch is more severe at junctions, roundabouts, complicated flyovers and built-up urban areas with complex route structures. These environments also decrease the level of performance achievable with GPS.

Therefore, Map Matching (MM) algorithms are usually used to reconcile the inaccurate locational data with inaccurate digital road network data. If both digital maps and vehicle location are perfectly accurate, the algorithm is simple and straightforward based on simply snapping the locational data to the nearest node or link

in the network. However, in most cases it is not possible to use such simple algorithms. Therefore, more complex MM algorithms are a required component for vehicle location and navigation systems.

The complexity of the MM algorithms depends on the nature of the application and the availability of data inputs. Previous research by the authors developed a simple MM algorithm appropriate for motorways and relatively sparse road networks (Quddus et al. 2003). The algorithm was also designed for low accuracy digital base maps where the source map resolution was 1:10,000 or below. The research presented in this paper builds on this previous work to develop a MM algorithm for all types of digital base maps and road networks. The new algorithm takes into account the error sources associated with the positioning sensors, the historical trajectory of the vehicle, the topological information on the road network (e.g., connectivity and orientation of links), and the heading and speed information of the vehicle, for the precise identification of the correct link on which the vehicle is traveling. Furthermore, an optimal estimation of the vehicle position is established by taking into consideration error sources associated with both the navigation systems and the digital map database.

2. LITERATURE REVIEW

MM algorithms are often used to determine the accurate position of a vehicle on a road map. Most of the formulated algorithms utilize navigation data from GPS, DR, or integrated GPS/DR and the digital road network data. One of the common assumptions found in the literature for implementing MM is that the vehicle is essentially constrained to a finite network of roads. Most of the studies (e.g., Zhao, 1997) also reported that the digital map used for MM must be quite robust in order to generate the position outputs in an error-free fashion. Procedures for MM vary from those using simple search techniques (Kim et al., 1996), to those using more complex mathematical techniques such as Kalman Filters (KF) (Tanaka et al., 1990).

The most commonly used geometric MM approach is based on a simple search concept. In this approach, each positioning point matches to the closest 'node' or 'shape point' in the network. This is also known as point-to-point matching (Bernstein and Kornhauser, 1996). A number of data structures and algorithms exist to identify the closest node (or shape point) from a given point in a network (e.g., Bentley and Maurer, 1980; Fuchs et al., 1980). These methods are easy to implement, although they are very sensitive to the way in which the network was digitized, hence leading to errors.

Another geometric MM approach is point-to-curve matching (e.g., Bernstein and Kornhauser, 1996; White et al., 2000; Taylor et al. 2001). In this approach, the positioning point from the navigation system is matched with the closest curve in the network. Each of the curves comprises line segments which are piece-

wise linear. Distance is calculated from the positioning point to each of the line segments. The line segment which gives the smallest distance is selected as the one on which the vehicle is assumed to be traveling. Although this approach gives better results than point-to-point matching, it does have several shortcomings that make it inappropriate in practice (in some cases), such as generating very unstable results in dense urban networks.

Another geometric approach is to compare the vehicle's trajectory against known roads. This is also known as curve-to-curve matching (Bernstein and Kornhauser, 1996; White et al., 2000). In this approach, firstly the candidate node using point-to-point matching is identified. Then, given a candidate node, piecewise linear curves are constructed from the set of paths that originate from that node. Secondly, piece-wise linear curves are then constructed using the vehicle's trajectory. The distance between the curve along the vehicle trajectory and the curve corresponding to the road network is then determined. The road arc which is closest to the curve formed from the vehicle trajectory is taken as the one on which the vehicle is apparently traveling. This approach is quite sensitive to outliers and depends on point-to-point matching, sometimes giving unexpected results (Greenfeld 2002).

Taylor et al. (2001) propose a novel method of map matching using GPS, height aiding from the digital road map and virtual differential GPS (VDGPS) corrections, referred to as the *road reduction filter (RRF)* algorithm. Due to the use of height aiding, the paper reports that one less satellite is required for the computation of the vehicle positions (i.e., height aiding removes one of the unknown parameters) using GPS. The initial matching process of this algorithm is based on the geometric curve-to-curve matching proposed by White (1991) which is quite sensitive to outliers. The proposed algorithm does not consider link connectivity information which could improve the performance of the algorithm especially in the initial matching process. It is well known that the vehicle heading from GPS is not good if the vehicle speed is low. Although the proposed algorithm is based on the bearing of the vehicle, there was no indication how to deal with the situation when the vehicle was stopped on a road segment for a few seconds. Moreover, the orthogonal projected location of the GPS fixes on the arc is used to determine the vehicle positions. However, Greenfeld (2002) described that the orthogonal projection of the position fixes on the arc are different from the actual location of the vehicle on the arc.

Greenfeld (2002) reviews several approaches for solving the map matching problem and proposes a weighted topological algorithm. The algorithm is based on assessing the similarity between the characteristics of the street network and the positioning pattern of the user. The paper reports that the procedure computes correct matches virtually everywhere. Quddus et al. (2003) tested this algorithm for a relatively sparse road network and concluded that sometimes the algorithm

identifies incorrect road segments. Greenfeld (2002) also suggests that additional research is required to verify the accurate performance of the algorithm and to make an accurate position determination on a given road segment.

Xu et al. (2002) proposed a new MM method based on intersection information stored in a map database. The method identified whether the vehicle is near intersections or between intersections or whether a turn is detected using DR sensors. However, the study did not take into account speed information and error sources associated with DR sensors. The algorithm also failed to deal with parallel roads and possible U-turns at junctions. Moreover, it does not determine the vehicle location on the road segment. This is one of the key improvements made by the algorithm developed in this paper.

3. ERRORS IN LAND VEHICLE NAVIGATION SYSTEMS

In a variety of transport telematics applications and services, the vehicle position on the road network is usually determined by the positioning systems, e.g., DR, GPS and the integrated GPS/DR system. Each of these navigation systems has various sources of error that lead to the need to apply MM. The next section briefly describes these navigation systems and their error sources.

3.1 Global Positioning System (GPS)

GPS is a satellite-based radio-navigation system owned and operated jointly by the US Department of Defense (DoD) and Department of Transportation (DoT). The system achieved full operational capability (FOC) in 1995 with a constellation of 24 active satellites (28 in March 2000). Theoretically, three or more GPS satellites are always visible from most points on the Earth Surface. The original objectives of GPS were the instantaneous determination of position and velocity (i.e., navigation), and the precise coordination of time (i.e., time transfer). GPS provides 24-hour, all-weather 3D positioning and timing all over the world, with a predicted horizontal accuracy of 22m (95%) [US DoD, 2001]. However, GPS suffers both systematic errors or biases and random noise e.g., satellite related errors such as clock bias and orbital errors, propagation related errors such as ionospheric refraction and tropospheric refraction, and receiver related errors such as multipath and clock bias.

3.2 Dead Reckoning (DR)

The DR is based on the integration of an estimated or measured displacement vector. Usually, it is composed of two or more sensors that measure the heading and displacement of a vehicle. A gyroscope is the main device used to measure the rate of rotation in an inertial navigation system such as DR. The odometer

uses the wheel rotation sensor to measure wheel revolutions. The wheel revolutions are then transformed into the distance traveled. Using time between two consecutive observations, the speed or velocity of the vehicle can also be determined. Errors associated with the rate gyroscope are gyro bias drift, gyro scale factor error, installation misalignment, temperature, and vibration and electro-mechanical properties of the operational environment. The most significant error is the bias drift that depends on the manufacturing process and the quality of the gyroscope. Factors affecting the odometer output accuracy are the scale factor error, status of the road and pulse truncation. The most significant error is the scale factor error that is caused by calibration error, tire wear and tear, tire pressure vibration and vehicle speed. The scale factor error is not significant over a short period of travel.

3.3 Integration of GPS and DR

In order to achieve the RNP in some areas e.g., urban canyons, streets with dense tree cover, and tunnels, GPS can be augmented with DR with the use of a Kalman Filter (KF) (Zhao et al., 2003). An understanding of the navigation errors involved is required to do this.

The KF is a set of mathematical equations that provides an efficient computational solution of the least-squares method. It is a linear minimum mean-square error (MMSE) filtering for combining noisy sensor outputs (i.e., GPS receivers, gyroscopes, odometers) to estimate the state of a system (i.e., position, velocity, heading, acceleration of a vehicle) with uncertain dynamics (i.e., unpredictable disturbances of the host vehicle, unpredictable changes in the sensor parameters). The nonlinear application of KF is known as the Extended Kalman Filter (EKF). An EKF algorithm can be used to estimate the optimal result of system states by integrating GPS and DR¹ (Figure 1).

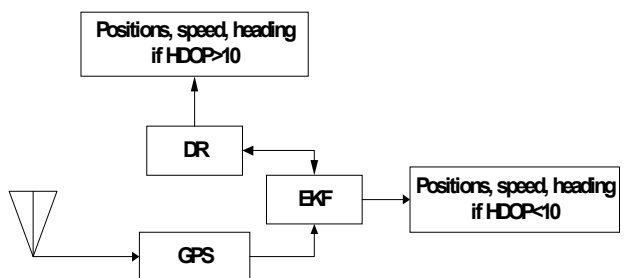


Fig. 1: Integrated navigation system for the vehicle dynamic model.

In this integrated navigation system, DR readings are calibrated when GPS is available using an EKF algorithm. If the GPS receiver suffers signal mask or the horizontal dilution of precision (HDOP) is greater than 10, which is an indication that navigation satellite

¹ The readers are referred to Zhao et al (2003) for a fuller description of the EKF algorithm

geometry is not good enough to get a high accuracy position, the calibrated DR readings are used to measure the state of the vehicle as shown in Figure 1.

4. THE PROPOSED MAP MATCHING ALGORITHM

4.1 Description of Algorithm Inputs

The inputs of the MM algorithm developed here are the locational data and topological information from the road network data. The locational data include position (e.g., easting and northing), speed, heading, and associated error variances. Locational data sources for this work included GPS, DR sensors (low cost gyro and odometer) and an integrated GPS/DR system employing an Extended Kalman Filter (EKF). A digital spatial road network database was the source of topological information. Error variances associated with the map resolution of the digital road network can also be taken as an input.

However, because of the current limitations of the digital road network data (e.g. no information on link connectivity) it was not possible to use it directly². A procedure to extract numerical link and node data from the spatial road network data was developed and used (Figure 2).

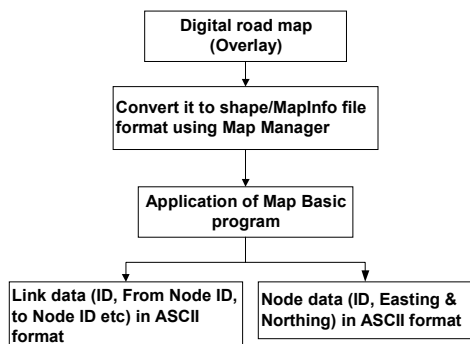


Fig. 2: Procedure to Extract Link and Node Data in ASCII format from a Digital Map.

4.2 The MM Algorithm execution stages

The algorithm makes use of the positioning data as well as the heading and speed information. Information on the historical trajectory of the vehicle is used to avoid sudden switching of the mapped locations between the unconnected road links. The topological aspects of the road network and the heading and speed information allow improvements in performance of the algorithm, especially at junctions. In addition, the physical location of the vehicle on the selected link is determined from an optimal estimation technique. Finally, the errors associated with the heading of the link (due to various error sources in the digital base map) and positioning sensors are applied to determine

the physical location of the vehicle on the link. There are two main stages of the algorithm, namely the identification of the actual link, and the determination of the vehicle position on the selected link. These are explained below.

4.2.1 Identification of the actual link

The most complex element of any MM algorithm is to identify the actual link among the candidate links (Greenfeld, 2002; Quddus et al. 2003). Two distinct processes are defined for the identification of the correct link, namely (a) the *initial matching process* (IMP) and (b) the *subsequent matching process* (SMP). The function of the IMP is to identify an initial correct link for an initial position fix. Since the vehicle is expected to travel on this initial road segment for a few seconds, the subsequent position fixes are matched to this road segment. Therefore, after successfully identifying a correct link for an initial GPS or GPS/DR fix, the SMP starts matching the subsequent position fixes. In the SMP, the fixes are matched to the same road segment identified in the IMP given that specified criteria³ are fulfilled. Otherwise, the algorithm goes back to the IMP for the identification of a new road segment for the last non-matched position fix. Both of these processes are explained below.

4.2.1.1 Initial Matching Process (IMP)

The IMP selects an initial road segment for the initial position fix. If an initial matching is incorrect then the subsequent matching will also be incorrect. Therefore, a sophisticated method is required for the IMP. The basic characteristic of the IMP is the use of an elliptical or rectangular confidence region around a position fix based on error models associated with GPS or GPS/DR. Road segments that are within the confidence region are taken as the pseudo candidate segments. If the confidence region does not contain any segments, then it is assumed that the vehicle is off the known road segments. In such a situation, the derived GPS or GPS/DR positions are used as the final locations of the vehicle. In a situation where the confidence region contains one or more pseudo candidate segments, a connectivity test or a filtering process is carried out based on the difference in heading between the pseudo candidate link and the derived vehicle heading to obtain the candidate road segments. If there is only one candidate segment, then the final selection process is very straightforward. However, in the case of more than one candidate segment, the link connectivity, vehicle heading relative to the candidate segments, closeness, and the historical information on vehicle location are used to select the most appropriate segment. In every application of the IMP, the algorithm selects a new road segment. The process is summarized in the flow chart in Figure 3.

² Note that digital spatial data specifically for transportation applications are beginning to emerge

³ These criteria are discussed in the SMP section

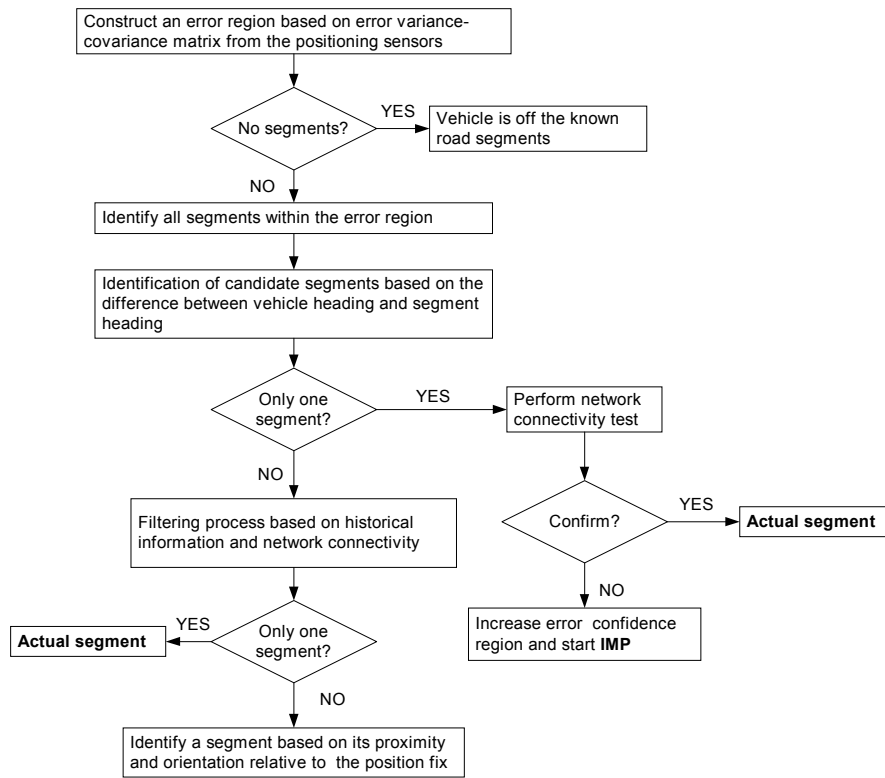


Fig. 3: The identification of the actual segment in the initial matching process

Many methods are available for calculating the error region around a position fix. Variance-covariance information associated with GPS receiver outputs is often used to define an error ellipse. If an EKF algorithm is used for the integrated navigation system (GPS/DR), the variance-covariance information is available as a by-product of the filter computation. According to Zhao (1997), the error ellipse can be derived as

$$a = \hat{\sigma}_0 \sqrt{1/2(\sigma_x^2 + \sigma_y^2) + \sqrt{(\sigma_x^2 - \sigma_y^2)^2 + 4\sigma_{xy}^2}} \quad (1)$$

$$b = \hat{\sigma}_0 \sqrt{1/2(\sigma_x^2 + \sigma_y^2) - \sqrt{(\sigma_x^2 - \sigma_y^2)^2 + 4\sigma_{xy}^2}} \quad (2)$$

$$\phi = \pi/2 - 1/2 \arctan\left(\frac{2\sigma_{xy}}{\sigma_x^2 - \sigma_y^2}\right) \quad (3)$$

where σ_x^2 and σ_y^2 are the positional error variances from the integrated GPS/DR, σ_{xy} is the covariance, a and b are the semi-major and semi-minor axis of the ellipse, ϕ is the orientation of the ellipse relative to the North (Figure 4a), and $\hat{\sigma}_0 (>1)$ is the expansion factor. The expansion factor is a term that compensates for the error associated with GPS due to orbital instability, atmospheric propagation, multipath, and receiver noise. To obtain a 99% confidence level, the value of the expansion factor should be taken as 3.03 (Zhao, 1997).

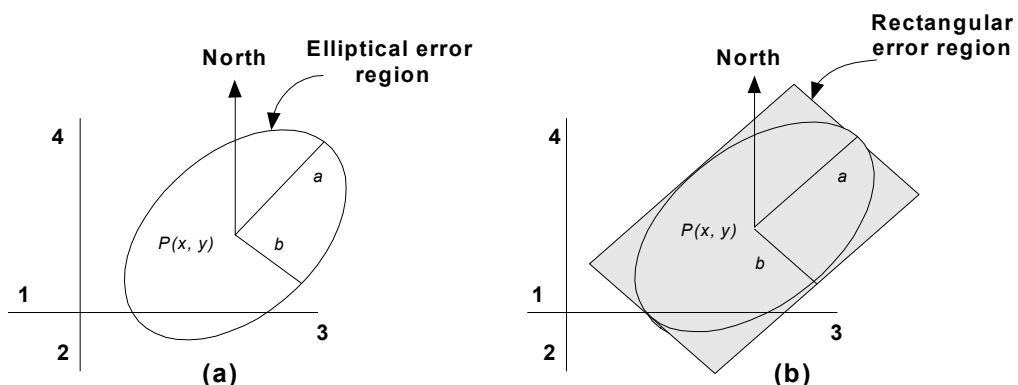


Fig. 4: Error ellipse and rectangular around a position fix.

In addition to the positioning sensor errors, there are also uncertainties associated with the digital road network data which could have errors due to plotting, errors in the original sources, measurement errors and processing mistakes. Hence, it is required to multiply the derived error region by another expansion factor to get a higher confidence level (Zhao, 1997). For simplicity, an error rectangular can be used in place of the error ellipse as shown in Figure 4(b). In the case represented by Figure 4, the IMP selects 'link 3' for both cases, as the initial road segment for the position fix $P(x, y)$.

4.2.1.2 Subsequent Matching Process (SMP)

The SMP is used to match the following position fixes on the previously selected road segment, which is identified using IMP. Several factors need to be considered for matching the subsequent position fixes to the link. These are the speed of the vehicle, whether there is a turning maneuver, or a maneuver through a junction. The speed of the vehicle needs to be taken into account since GPS or GPS/DR derived headings are not sufficiently accurate when the speed is low. On the other hand, the detection of a turning maneuver or a maneuver through a junction is a good indication that the vehicle no longer located on the original segment. If the vehicle speed is lower than the threshold for the minimum speed and there is no indication of any maneuvering through a junction by the vehicle, the SMP process continues. In such cases, the vehicle heading needs to be re-calculated to be equal to the heading of the road segment obtained from the map database. The new calculated vehicle heading is used to identify any turning maneuver for the next position fix. Field tests are necessary to determine a threshold for the minimum speed and this is explained in the next section.

In case of speeds higher than the threshold minimum speed, the SMP also continues if there is neither a turning maneuver nor junction crossing. The criterion to determine a turning maneuver is also explained in detail in the next section with some field test results. The decisive factor to determine whether the vehicle crosses any junction (in the case of maneuvers through a junction) can be determined from the relative position of the current GPS or GPS/DR fix compared to the previously selected road segment. The complete flow chart for the identification of the link on which a vehicle is traveling is presented in Figure 5.

The MM algorithm makes use of the vehicle heading to identify whether there is a turning maneuver at a junction. A turning maneuver is an indication that the vehicle may have switched road segments. Therefore, the algorithm searches for a new road segment (using IMP) if a turning maneuver is confirmed. However, at low speed the error associated with vehicle heading is usually unacceptably low. Hence, it is essential to determine the minimum speed at which the MM algorithm should *not* rely on vehicle heading (either from GPS or integrated GPS/DR).

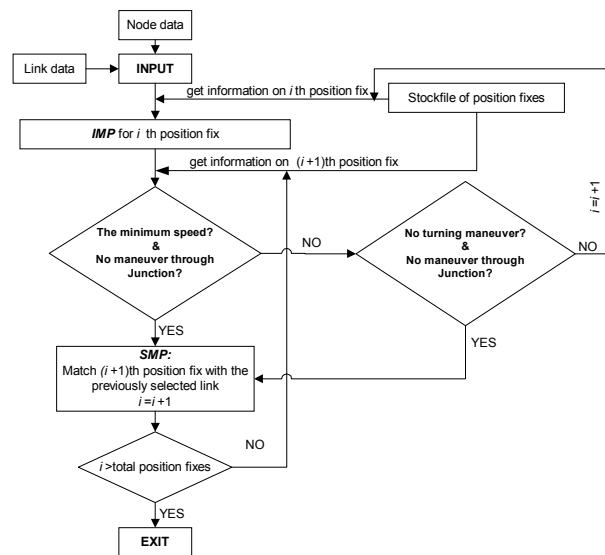


Fig. 5: Flow chart for true road segment identification.

4.2.1.3 Determination of a turning maneuver and the minimum speed

A field test was carried out to determine the minimum speed at which GPS or GPS/DR derived vehicle headings are not reliable. The test vehicle was driven on known road segments. Since the vehicle traveled on known road segments, the actual vehicle headings were calculated from the digital map database. The absolute deviation of vehicle heading was obtained from the difference between the calculated actual heading and the observed/estimated GPS or GPS/DR heading. The deviation of heading was then plotted against the corresponding vehicle speed (see Figure 6) for both GPS and GPS/DR system. For this case the difference in heading was always less than 30 degrees when the vehicle speed exceeded 3 m/sec (i.e., 10.8 km/hr) for both GPS and the GPS/DR systems i.e., the vehicle headings derived from the GPS and the road segment heading on which the vehicle is travelling is correlated when the vehicle speed is above 10.8 km/hr⁴. The satellite geometry was good since HDOP was always less than 2.0. Therefore, the algorithm can rely on the vehicle heading information, which is useful for determining a turning maneuver, if the vehicle speed is greater than 3 m/sec. Hence the minimum speed threshold is set to 3m/sec (i.e., 10.8 km/hr). It is worthwhile to note that the threshold for the minimum speed may vary according to the types of GPS receivers and their error characteristics.

⁴ Taylor et al. (2001) reports that the correlation is low when the vehicle is travelling at 8 km/hr or below.

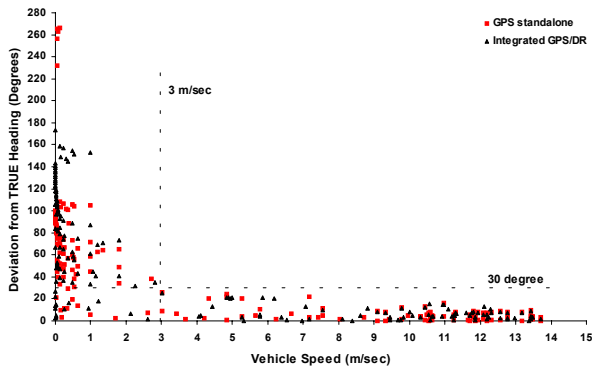


Fig. 6: The absolute deviation of vehicle heading vs speed.

In order to find out the threshold for the vehicle heading that could be used for detecting a turning maneuver, it is also necessary to know how the vehicle heading changes on a straight road segment. To determine this, another field test was carried out on a straight road segment. The vehicle was intentionally driven with a lot of overtaking maneuvers to examine the effects on heading changes. Figure 7 shows the change in vehicle headings on a typical straight road when the speed is greater than 3 m/sec. In all cases, HDOP was less than 2.0. The maximum difference between observed vehicle headings was 20 degrees for GPS and 15 for GPS/DR. The reason for such a large difference in heading on a straight road may be due to the overtaking maneuvers. However, neither an increasing nor decreasing trend was observed for the heading.

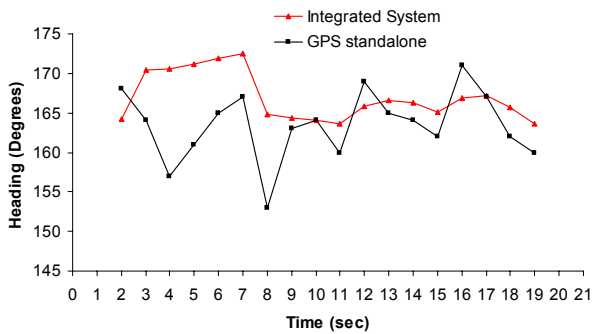


Fig. 7: Characteristics of GPS/DR and GPS headings when the vehicle is traveling on a straight road.

Another field test was carried out to examine the change in vehicle headings during a turning maneuver at junction. This test was also useful for determining the time needed to complete a turning maneuver. Figure 8 shows the changes in observed vehicle heading during a right turning (British-style) i.e., left-turn elsewhere maneuver of a vehicle at a four-legged junction when the vehicle speed is above the minimum speed and HDOP less than 2.0. Clearly, there is a trend (in this case an increasing trend) of heading during the turning maneuver. Time to complete a right- or left-turning maneuver usually depends on speed and

the size of the junction. In this case, the time to complete a right-turning maneuver was 4 sec.

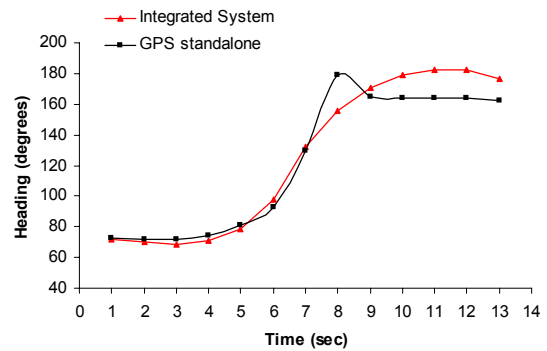


Fig. 8: Characteristics of GPS and GPS/DR headings during a right turning maneuver of a vehicle at junction.

Based on these above test results, the following conditions satisfy a turning maneuver (left, right or U-turn) of a vehicle at a junction.

- Increasing or decreasing trend in heading for about 2 to 5 sec
- Absolute difference in heading between the current and the last fix (assumed as α) is more than 30 degrees (for both GPS and GPS/DR)
- Absolute difference in heading between the current and the second last fix (assumed as β) is more than 35 degrees (for both GPS and GPS/DR)

4.2.2 Determination of Vehicle Location on the Selected Link

Assuming that the correct link has been identified as per the IMP and/or SMP, the physical location of the vehicle on the link can be determined in two ways with the available data. One way is to use map data and vehicle speed from the positioning sensors and the other is to adopt the perpendicular projection of GPS or GPS/DR fix on to the link. Since both methods are associated with errors, an optimal estimation procedure is needed to determine the final location of the vehicle on the road segment.

The azimuth of the selected road segment and the vehicle speed (v) from the positioning unit can be used to calculate the vehicle position on a road segment. Suppose P^t and P^{t+1} represent the vehicle position on a link at time t and $t+1$ respectively (Figure 9). The initial easting and northing of the vehicle at point P^t is known. From the bearing of the link (i.e., θ) and speed of the vehicle at P^{t+1} , the increment in easting and northing can be obtained as follows:

$$\left. \begin{aligned} \Delta E_i &= (v) \sin \theta \\ \Delta N_i &= (v) \cos \theta \end{aligned} \right\} \quad (4)$$

Therefore, the position of the vehicle at point P^{t+1} can be calculated as follows:

$$\left. \begin{aligned} E_{i+1} &= E_i + \Delta E_i \\ N_{i+1} &= N_i + \Delta N_i \end{aligned} \right\} \quad (5)$$

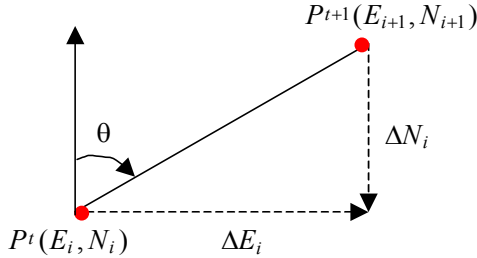


Fig. 9: Determination of vehicle position using map data and vehicle speed.

The other method for determining position is from the positioning sensor (Figure 10). Suppose the navigation unit locates the vehicle at point P^S with easting, e_s and northing, n_s . The projected easting (e_2) and northing (n_2) on the link can be obtained as follows:

$$\left. \begin{aligned} e_2 &= \frac{(x_2 - x_1)[E_S(x_2 - x_1) + N_S(y_2 - y_1)] + (y_2 - y_1)(x_1 y_2 - x_2 y_1)}{(x_2 - x_1)^2 + (y_2 - y_1)^2} \\ n_2 &= \frac{(y_2 - y_1)[E_S(x_2 - x_1) + N_S(y_2 - y_1)] - (x_2 - x_1)(x_1 y_2 - x_2 y_1)}{(x_2 - x_1)^2 + (y_2 - y_1)^2} \end{aligned} \right\} \quad (6)$$

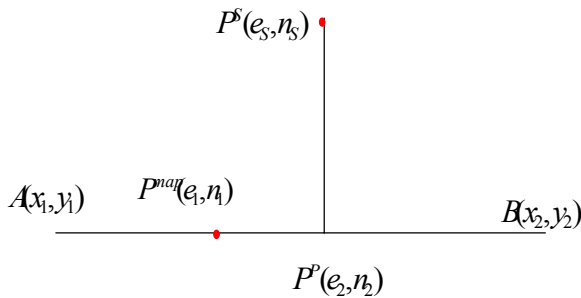


Fig. 10: The vehicle location on a particular road segment from two methods.

In Figure 10, the identified road segment for a position fix P^S is AB. The vehicle location P^{map} (e_1, n_1) on AB is measured from the digital base map and speed from the navigation system and P^P (e_2, n_2) is measured from the perpendicular projection of P^S on AB. Both techniques have random and unbiased measurement errors.

The easting coordinates from these two methods are denoted by e_1 and e_2 , and can be represented by the following equations

$$e_1 = e + \omega_1 \quad \text{and} \quad e_2 = e + \omega_2 \quad (7)$$

where e is the optimal estimate of easting, ω_1 and ω_2 are errors associated with the map data and the positioning unit respectively with $E(\omega_1 \omega_2) = \rho \sigma_1 \sigma_2$ in which ρ is the correlation coefficient between error terms and σ_1 and σ_2 are the standard deviation of ω_1 and ω_2 respectively. Since there is no more information available about the estimate of e , according to Gelb (1979) the optimal estimate is simply the linear function of the measurements in the form

$$\hat{e} = k_1 e_1 + k_2 e_2 \quad (8)$$

where k_1 and k_2 still need to be specified and are independent of e . The estimation error is denoted by

$$\tilde{e} = \hat{e} - e \quad (9)$$

The criterion of optimality is to minimize the mean square of \tilde{e} . Moreover, the estimate needs to be unbiased since k_1 and k_2 are independent of the value of e . This holds when

$$E[\tilde{e}] = E[k_1(e + \omega_1) + k_2(e + \omega_2) - e] = 0 \quad (10)$$

By applying, $E[\omega_1] = E[\omega_2] = 0$ and $E[e] = e$, equation (10) becomes

$$k_1 e + 0 + k_2 e + 0 - e = 0, \quad \text{i.e.,} \quad k_1 = 1 - k_2 \quad (11)$$

The mean square error is

$$\begin{aligned} E[\tilde{e}^2] &= E[((k_1(e + \omega_1) + (1 - k_1)(e + \omega_2)) - e)^2] \\ &= k_1^2 \sigma_1^2 + (1 - k_1)^2 \sigma_2^2 + 2k_1(1 - k_1)\rho\sigma_1\sigma_2 \end{aligned} \quad (12)$$

Differentiating equation (12) with respect to k_1 and setting the result to zero yields

$$k_1 = \frac{\sigma_2^2 - \rho\sigma_1\sigma_2}{\sigma_1^2 + \sigma_2^2 - 2\rho\sigma_1\sigma_2} \quad (13)$$

From equation (11), it can be shown that

$$k_2 = \frac{\sigma_1^2 - \rho\sigma_1\sigma_2}{\sigma_1^2 + \sigma_2^2 - 2\rho\sigma_1\sigma_2} \quad (14)$$

The optimal estimation of the easting coordinate is therefore obtained from equation (8) as,

$$\hat{e} = \left(\frac{\sigma_2^2 - \rho\sigma_1\sigma_2}{\sigma_1^2 + \sigma_2^2 - 2\rho\sigma_1\sigma_2} \right) e_1 + \left(\frac{\sigma_1^2 - \rho\sigma_1\sigma_2}{\sigma_1^2 + \sigma_2^2 - 2\rho\sigma_1\sigma_2} \right) e_2 \quad (15)$$

and hence equation (12) becomes

$$E[\tilde{e}^2] = \frac{\sigma_1^2 \sigma_2^2 (1 - \rho^2)}{\sigma_1^2 + \sigma_2^2 - 2\rho\sigma_1\sigma_2} \quad (16)$$

where $\sigma^2 = E[\tilde{e}^2]$ is the variance of the error term \tilde{e} . Then equation (16) can be rewritten as

$$\sigma^2 = \frac{\sigma_1^2 \sigma_2^2 (1 - \rho^2)}{\sigma_1^2 + \sigma_2^2 - 2\rho\sigma_1\sigma_2} \quad (17)$$

Similar to equation (15), the optimal estimation of the northing coordinate can be determined from

$$\hat{n} = \left(\frac{\sigma_2^2 - \rho\sigma_1\sigma_2}{\sigma_1^2 + \sigma_2^2 - 2\rho\sigma_1\sigma_2} \right) n_1 + \left(\frac{\sigma_1^2 - \rho\sigma_1\sigma_2}{\sigma_1^2 + \sigma_2^2 - 2\rho\sigma_1\sigma_2} \right) n_2 \quad (18)$$

Assuming that there is no correlation between the error terms from these two measurement techniques i.e., $E[\omega_1\omega_2] = 0$ and $\rho = 0$ then the optimal estimation is obtained from (15) and (18) by taking $\sigma_1 = \sigma_{map}$, $\sigma_2 = \sigma_{ps}$, $e_1 = e_{map}$ and $e_2 = e_{ps}$ where subscript *ps* indicates positioning sensor

$$\hat{e} = \left(\frac{\sigma_{ps}^2}{\sigma_{map}^2 + \sigma_{ps}^2} \right) e_{map} + \left(\frac{\sigma_{map}^2}{\sigma_{map}^2 + \sigma_{ps}^2} \right) e_{ps} \quad (19)$$

$$\hat{n} = \left(\frac{\sigma_{ps}^2}{\sigma_{map}^2 + \sigma_{ps}^2} \right) n_{map} + \left(\frac{\sigma_{map}^2}{\sigma_{map}^2 + \sigma_{ps}^2} \right) n_{ps} \quad (20)$$

the error variance associated with \hat{e} or \hat{n} can now be expressed as (from equation 17)

$$\frac{1}{\sigma_{mm}^2} = \frac{1}{\sigma_{map}^2} + \frac{1}{\sigma_{ps}^2} \quad (21)$$

where σ_{mm}^2 is the error variance associated with optimal estimation of \hat{e} or \hat{n} . Note from equation (21) that σ_{mm}^2 is less than either σ_{map}^2 or σ_{ps}^2 . That is, the uncertainty in estimation of the vehicle position using optimal estimation is decreased by combining two measurement methods.

5. TESTING OF THE ALGORITHM USING REAL DATA

The testing of the MM algorithm is essential to evaluate its performance in real-world applications. A comprehensive field test is required to collect the positioning data from various road environments. This is necessary because the performance of MM algorithms depend on road network characteristics.

Positioning data to test the performance of the algorithm was obtained from a comprehensive field test in Central London in January 2002. A vehicle was equipped with a navigation platform consisting of a 12-channel single frequency GPS receiver, a low-cost MEMS rate gyroscope and the interfaces required to connect to the vehicle speed sensor (odometer) and back-up indicator. The route in London was chosen carefully to have a good mix of important spatial urban characteristics including open spaces, urban canyons, tall buildings, tunnels, bridges, and potential sources of electromagnetic interference. The duration of data collection was about 4 hrs.

The positioning data (easting and northing), speed, and heading were collected at a one second interval directly from the GPS receiver. Corresponding data together with the associated error variances were also obtained from the integrated navigation system (GPS/DR) employing an EKF algorithm.

In order to see the level of coverage and the accuracy offered by GPS and the integrated system, the position fixing data was overlaid onto a high-resolution digital road network base map (Figure 11). The statistics generated from the field data show that GPS coverage was obtained for 90% of the mission duration, while that of the integrated system was 100%. The longest period of GPS outage was found to be 100s. It was also found that the integrated (GPS/DR) system performs better than standalone GPS in providing continuous positioning with an accuracy of better than 50m (Zhao et al., 2003). In general, the position accuracy in open areas was better than in the built-up areas.

Some parts of the test route were examined in greater detail. Figure 12 shows the vehicle travelling inside the Blackwall tunnel where there was a GPS outage for a period of 100s. It was found that 49% of the fixes were within 10m of the centreline of the road and 100% of the fixes were within 30m. This is a measure of the performance of the dead reckoning unit working on its own but using calibration factors derived when GPS position fixing capability was available.

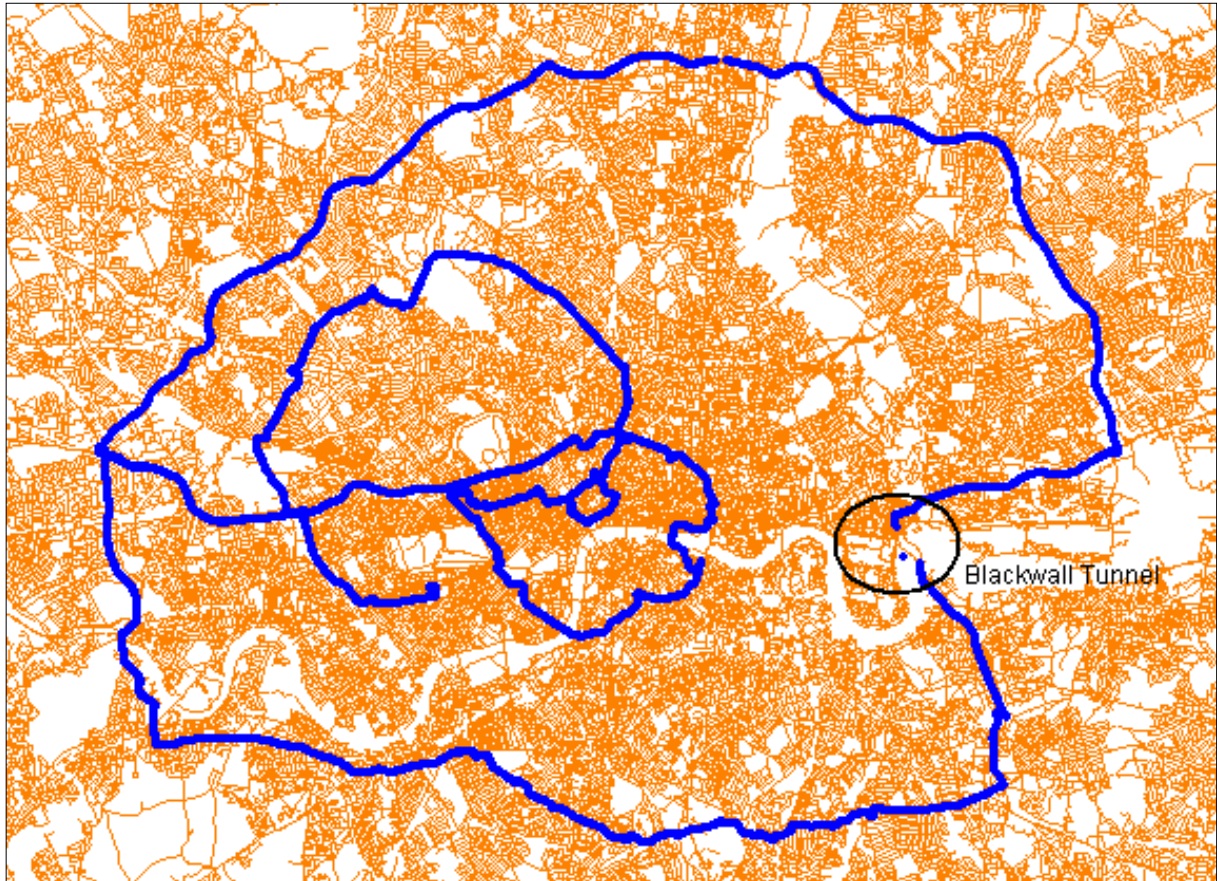


Fig. 11: Vehicle Trajectory from Position Fixing Data from GPS in Central London.

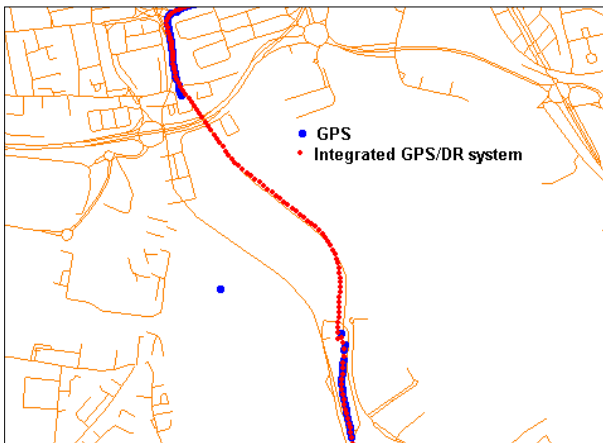


Fig. 12: Travelling inside Blackwall Tunnel.

The MM algorithm can be used with locational data from either GPS or the integrated GPS/DR system and any large-scale digital spatial road network data⁵ (source scale 1:1 to 1: 24,000). In order to see the performance of the algorithm, various scenarios were tested. Since the locational data from the integrated GPS/DR system are more reliable than GPS (Zhao et al. 2003), the performance of the algorithm has been tested using the navigation data from the integrated GPS/DR

⁵ Maps for ITS (i.e., Transport telematics) applications may be at scales between 1:5,000 to 1:10,000 in cities and at smaller scales along the major roads outside metropolitan areas (Zhao, 1997).

system. A large-scale digital spatial road network data (source scale 1:2500) supplied by Saturn Technologies UK is used to test the performance of the algorithm.

The algorithm was tested for various scenarios with different network characteristics and with different traffic maneuvers. These were a complex urban road network where the distance between roads was very small (Figure 13), a left-turning maneuver at a complex junction (Figure 14), a congested road with low speeds at mid-block (Figure 15), waiting at a traffic light (Figure 16), and traveling through a roundabout (Figure 17).

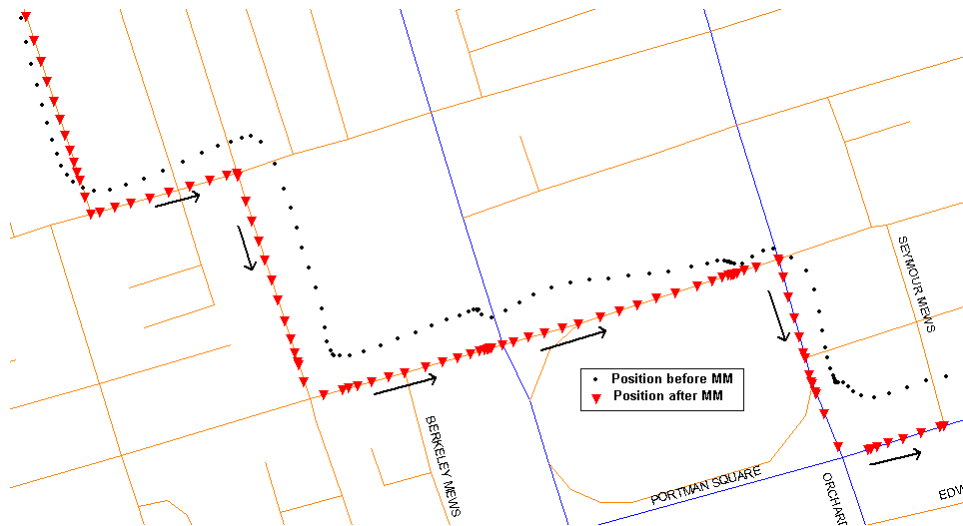
Each of the black round dots in the Figures (13-17) represents the vehicle position before MM. The arrow symbols in the figures show the path followed by the vehicle on the network. Note that in most cases the dot points deviate up to 40 m (Figure 18) from the actual route taken by the vehicle (for Figures 15 and 16 only). This may be due to positioning errors in the integrated system (although 100% of all position fixes were within 50m of the road center-line).

The semi-major axis (i.e., a) and the semi-minor axis (i.e., b) of the error ellipse (see equation 1) can be seen to be between 20m to 50m and 15m to 46m respectively whenever IMP is required. The rectangular confidence region constructed from the major and minor axis of the error ellipse always contains one or more road segments. This is an indication that the vehicle was not traveling off the known road segments. The

threshold values for the minimum speed is taken as 3m/sec, α is taken as 30° , and β is taken as 35° . These values are used to detect any maneuvers at junctions. 100% correct link identification is achieved for all scenarios.

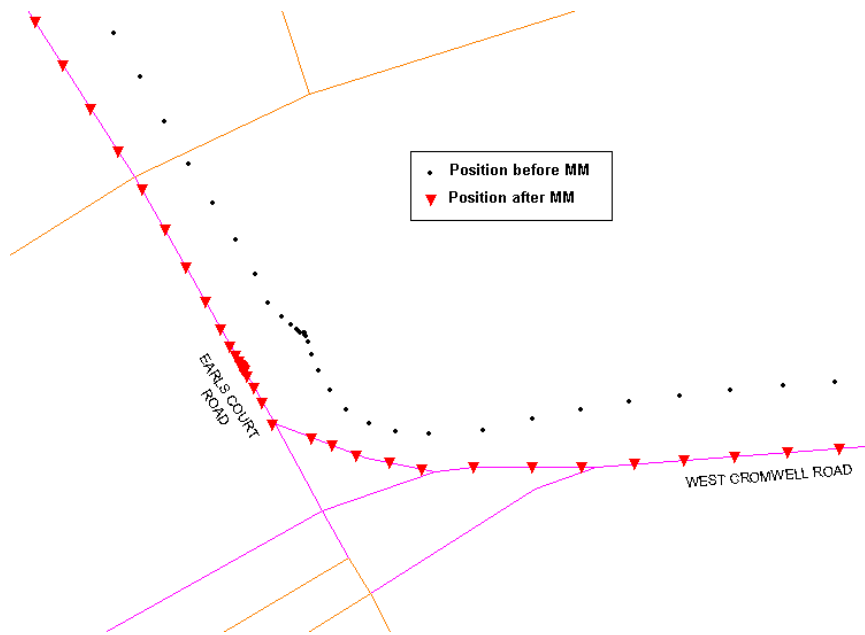
Each of the triangular symbols on the road segments represents the vehicle position after MM. The position of the vehicle on a selected road segment was

estimated using two positioning methods (estimation using map data with the vehicle speed information from the positioning unit and the other is from the orthogonal projection of the GPS/DR fix on the road segment). Since there is no correlation between the error terms in these two methods, equations (19) and (20) were used for the optimal estimation of easting and northing coordinates respectively.



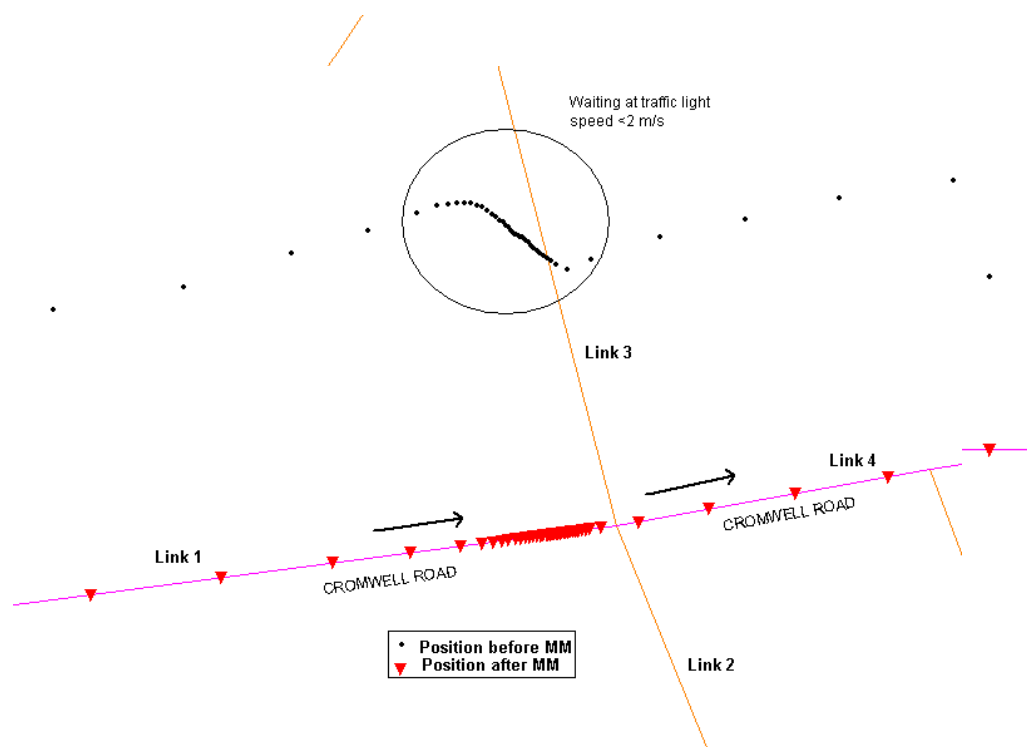
(Presentation map scale 1 cm : 20 m)

Fig. 13: Map matching results on complex urban road network.

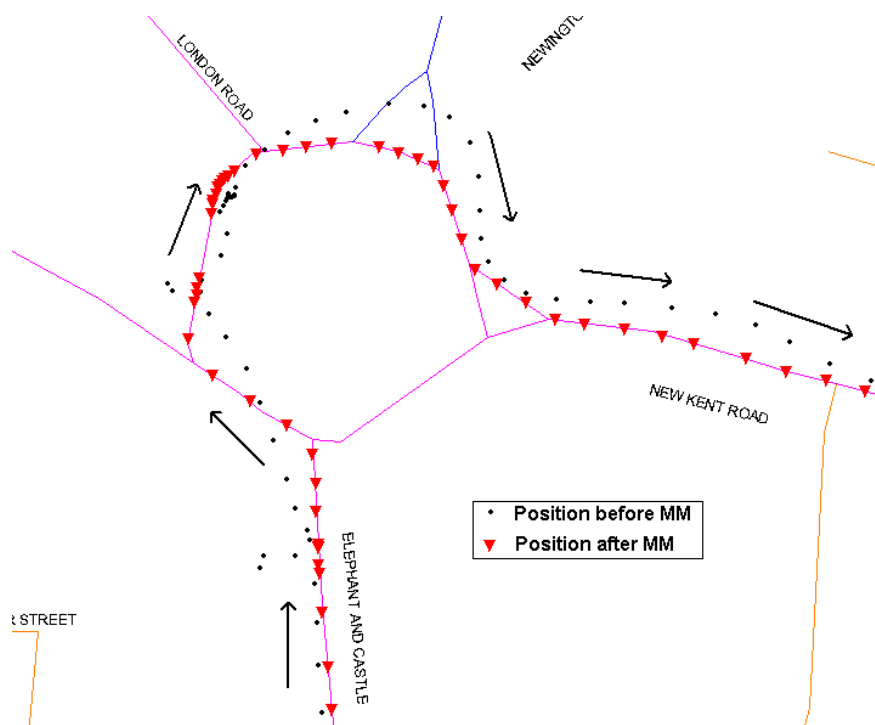


(Presentation map scale 1 cm : 10 m)

Fig. 14: Map matching results on left-turn maneuvering at complex junction.



(Presentation map scale 1 cm : 15 m)
 Fig. 16: Map matching results during waiting at traffic light.



(Presentation map Scale: 1cm: 24m)
 Fig. 17: Map matching results at roundabout.

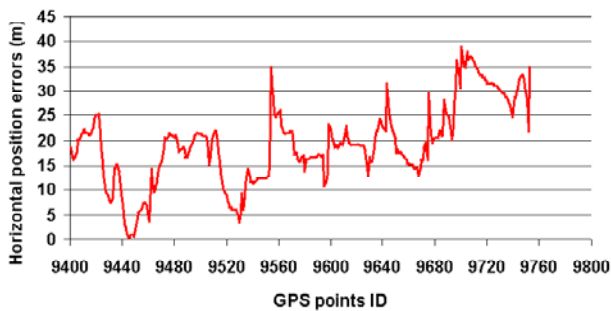


Fig. 18: The deviation of positions (for Figure 15 and 16 only) from the road centre line.

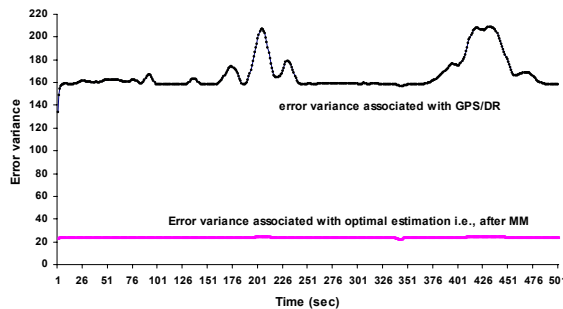


Fig. 19: Comparisons of error variances between GPS/DR and MM results.

Figure 19 shows the variation of error variances (easting) with time for both the integrated GPS/DR system and MM results. The error variances associated with the integrated GPS/DR system are much higher than that from MM. The average standard deviation (i.e., error sigma) in the GPS/DR system is 10 to 16m whereas it is 4 to 5m after MM. The northing component of the position also gives similar ranges of error variance. Therefore, it can be said that the MM algorithm improves the uncertainty associated with the integrated GPS/DR system as was indicated by equation (21). Initial measure of accuracy revealed 100% link identification for all the position fixes. Further work is on going to quantify positional accuracy for each map-matched point.

6. CONCLUSION

The integration of low cost DR sensors and GPS can be achieved employing an EKF algorithm. This integrated navigation system gives continuous vehicle position fixes (including urban canyons, streets with dense tree cover and tunnels). However, the vehicle positions derived from the integrated system do not always map to the actual vehicle position. This paper has developed and demonstrated a Map Matching (MM) algorithm to accurately display vehicle location on a GIS-based digital map.

Probabilistic approaches were applied for both identification of the actual road segment on which the vehicle was traveling and the determination of the vehicle position. The algorithm was tested on various complex urban roadways and traffic scenarios with a relatively high-resolution digital map of the road

network. The algorithm achieved correct matching 100% of the time covering sparse and complex networks. The algorithm not only reconciles the inaccurate locational data with an inaccurate digital road network data but also improves the uncertainty associated with the determination of the vehicle position. The standard deviation of map matched positions was reduced to 4 to 5m for the easting and northing coordinates respectively, from of 10 to 16m as determined from the integrated (GPS/DR) system output.

It should be noted that although the algorithm develop was tested off-line, it can easily be implemented to work in real-time. The next step of this study is to validate the performance of the algorithm using a higher accuracy reference (truth) of the vehicle trajectory as determined by the carrier phase observable from GPS. This will also enable the realization of a reliability indicator for map matching.

7. REFERENCES

- BENTLEY, J.L., M., H.A., 1980. Efficient worst-case data structures for range searching. *Acta Inf.* 13, pp. 155-168.
- BERNSTEIN D., KORNHAUSER A., 1996. **An introduction to map matching for personal navigation assistants.** New Jersey TIDE Center <http://www.njtude.org/reports/mapmatchintro.pdf>.
- GREENFELD, J.S., 2002. Matching GPS observations to locations on a digital map. In **Proceedings of the 81th Annual Meeting of the Transportation Research Board**, Washington D.C.
- FUCHS, H., KEDEM, Z.M., NAYLOR, B.F., 1980. On visible surface generation by a priori tree structures. *Comput. Graphics*, 14, pp. 124-133.
- GELB, A. 1979. **Applied Optimal Estimation.** The MIT press.
- JO, T., HASEYAMAI, M., KITAJIMA, H., 1996. A map matching method with the innovation of the Kalman filtering. *IEICE Trans. Fund. Electron. Comm. Comput. Sci.* E79-A, pp 1853-1855.
- KIM, J.S., LEE, J.H., KANG, T.H., LEE, W.Y., KIM, Y.G., 1996. Node based map matching algorithm for car navigation system, **Proceeding of the 29th ISATA Symposium**, Florence, Vol. 10, pp 121-126.
- KRAKIWSKY, E.J., HARRIS, C.B., WONG, R.V.C., 1988. A Kalman filter for intrgrating dead reckoning, map matching and GPS positioning. In: **Proceedings of IEEE Position Location and Navigation Symposium**, 39-46.

- OCHIENG, W.Y., SAUER, K., 2001. Urban road transport navigation requirements: performance of the global positioning system after selective availability. **Transportation Research Part C**, 10, 171-187.
- QUDDUS, M.A., OCHIENG, W.Y., ZHAO, L., NOLAND R.B., 2003. A general map matching algorithm for transport telematics applications. **GPS solutions**, 7(3), 157-167.
- SCOTT, C.A., DRANE, C.R., 1994. Increased accuracy of motor vehicle position estimation by utilizing map data, vehicle dynamics and other information sources. In: **Proceedings of the Vehicle Navigation and Information Systems Conferences**, 585-590.
- TANAKA, J., HIRANO, K., ITOH, T., NOBUTA, H., TSUNODA, S., 1990. Navigation system with map-matching method. **Proceeding of the SAE International Congress and Exposition**, pp 40-50.
- TAYLOR, G., BLEWITT, G., STEUP, D., CORBETT, S., CAR, A., 2001. Road reduction filtering for GPS-GIS navigation. **Proceedings of 3rd AGILE Conference on Geographic Information Science**, Helsinki, Finland, pp. 114-120.
- US DOD. 2001. **Global Positioning System Standard Positioning Service Performance Standard. Assistant secretary of defense for command, control, communications, and intelligence.**
- XU, A.G., YANG, D.K., CAO, F.X., XIAO, W.D., LAW, C.L., LING, K.V., AND CHUA, H.C. 2002. Prototype design and implementation for urban area in-car navigation system. In **Proceedings of IEEE 5th International Conference on Intelligent Transportation Systems**, 3-6 September, Singapore.
- WHITE M. 1991. **Car navigation systems**. In Maguire D J, Goodchild M F and Rhind D W (eds) **Geographical Information Systems: Principles and Applications**. Harlow, Longman: 115-25.
- WHITE, C.E., BERNSTEIN, D., KORNHAUSER, A.L., 2000. **Some map matching algorithms for personal navigation assistants**. **Transportation Research Part C** 8, 91-108.
- ZHAO, Y., 1997. **Vehicle Location and Navigation System**. Artech House, Inc., MA.
- ZHAO, L., OCHIENG, W.Y., QUDDUS, M.A AND NOLAND, R.B., 2003. An Extended Kalman Filter algorithm for Integrating GPS and low-cost Dead reckoning system data for vehicle performance and emissions monitoring. **The Journal of Navigation**, 56, 257-275.

Invited paper